

FINITE ELEMENT SIMULATIONS OF SOLIDIFICATION WITH A FIXED MESH FRONT TRACKING METHOD

Pinghua Zhao and Juan C. Heinrich

Department of Aerospace and Mechanical Engineering
The University of Arizona, Tucson, AZ, 85721, USA

ABSTRACT

Moving boundary problems in which the location of an interface must be determined as part of the solution arise in many scientific and engineering applications, one of utmost importance of which is crystal growth. There are three basic ways to address these problems numerically: (1) Fixed grid methods based on a finite difference or finite element discretization in which the basic computational mesh is fixed and the interface is tracked using either a field variable or a discrete set of points that define it. (2) Adaptive grid methods also based on finite differences or finite elements in which the interface is described by grid points in the computational mesh. (3) Boundary integral methods in which the problem is cast in the form of an integral representation of the interface. Here, we present a fixed grid method based on finite elements where the interface is described by a set of tracer points. We solve the conservation equations of energy and solute transport and pay special attention to the accurate calculation of the interface velocity. We also show that the method is second-order accurate. Example applications including the solidification of a binary alloy under a temperature gradient and the growth of dendrites into an under-cooled liquid are presented.

INTRODUCTION

The understanding of dendritic growth requires a detailed description of the heat and solute transport in the vicinity of the dendrite tips as well as the factors that control the stability of the shape of the dendrites. The modeling of the heat and solute transport is complicated by the presence of the solid-liquid interface. The position of the interface must be calculated as part of the problem solution and interface conditions must be satisfied, resulting in a highly nonlinear problem that is very sensitive to numerical error and is prone to numerical instability. The difficulties involved in the numerical simulation of the "sharp interface" problem led to the development of "phase-field" methods over the last 20 years [1,2]. The phase-field methods are diffused interface models that introduce a continuous transition between the two phases across a thin layer of finite thickness. An additional variable called the phase field is introduced that identifies the phase. This has the advantage that the location of the interface does not have to be explicitly determined. On the other hand, an extra equation for the phase field that contains very thin regions with large spatial gradients must be solved. A drawback of this method is that it cannot be easily modified to treat other types of interface problems of engineering interest.

Fixed-mesh methods that solve the sharp interface problem have been proposed over the last 10 years [3, 4]. These models are based on finite-difference approximations to the governing equations and are only first-order accurate. Finite element models have also been published [5, 6], but these are based on adaptive meshes.

In this work, we present a fixed-mesh finite-element model with interface tracking. The interfaces are described by a set of marker points that move in time according to the interface dynamics. During the development of the method, it was found that most existing models for the phase change problem suffer from an inability to calculate the interface velocity without introducing severe oscillations. Special techniques are developed that greatly reduce these oscillations, even though it does not appear to be possible to eliminate them completely. Due to space constraints, we will present some of the basic features of the method in a one-dimensional context only. The reader should keep in mind that, because the interface dynamics occur along the direction normal to the interface, most of the concepts can be applied unmodified to two and three dimensions.

PROBLEM FORMULATION

We consider the solidification of a binary alloy assuming that diffusion is the only mechanism for heat and mass transport. The energy conservation equation is

$$\eta \frac{\partial T_s}{\partial t} = \Lambda \nabla^2 T_s \quad \text{in the solid phase} \quad (1a)$$

$$\frac{\partial T_l}{\partial t} = \nabla^2 T_l \quad \text{in the liquid phase} \quad (1b)$$

and at the solid-liquid interface

$$T_s = T_l \quad (2a)$$

$$\Lambda \frac{\partial T_s}{\partial n} - \frac{\partial T_l}{\partial n} = \left(\frac{1}{St} - \gamma (T_l - T_m) \right) V \quad (2b)$$

The solute concentration equations are

$$\frac{\partial C_s}{\partial t} = \frac{1}{Le_s} \frac{\partial^2 C_s}{\partial x^2} \quad \text{in the solid phase} \quad (3a)$$

$$\frac{\partial C_l}{\partial t} = \frac{1}{Le_l} \frac{\partial C_l}{\partial x^2} \quad \text{in the liquid phase} \quad (3b)$$

At the interface, the liquid concentration satisfies

$$\left(-\frac{1}{Le_l} \nabla C_l \right) \cdot \hat{n} = (1-k)(C_l - \hat{C}) V \quad (4)$$

The interface condition for the solid phase depends on whether the solute concentration at the interface is eutectic or hypo-eutectic. If it is not eutectic, we have

$$C_s = kC_l \quad \text{at the interface} \quad (5a)$$

Otherwise,

$$C_s = C_l + \left(\frac{1}{Le_l(1+\beta)} \right) \hat{n} \cdot \nabla C_l \quad (5b)$$

The equations have been nondimensionalized using H as the reference length, $\tau = H^2/\alpha_\ell$ as the reference time, $T = (T^* - T_m)/\Delta T$, and $C = (C^* - C_0)/(C_E - C_0)$, where the asterisk (*) indicates a dimensional quality.

The parameters are $\eta = \rho_s c_{p_s}/\rho_\ell c_{p_\ell}$, $\Lambda = \alpha_s/\alpha_\ell$, $St = c_{p_\ell} \Delta T/L$, $\gamma = (c_{p_s} - c_{p_\ell})/c_{p_\ell}$, $\hat{C} = C_0/(C_E - C_0)$, $Le_s = \alpha_\ell/D_s$, $Le_\ell = \alpha_\ell/D_\ell$, and $\beta = (\rho_s - \rho_\ell)/\rho_\ell$, where $\alpha_\ell = \kappa_\ell/\rho_\ell c_{p_\ell}$ and $\alpha_s = \kappa_s/\rho_\ell c_{p_\ell}$.

Here, the subscripts s and ℓ refer to the solid and liquid phases, respectively; ρ is density; C_p is specific heat; V is the interface velocity; κ is thermal conductivity; D is mass diffusivity; k is the equilibrium partition ratio; T_{m_0} is the initial melting temperature of the alloy; T_E is the eutectic temperature; C_0 is the initial concentration; C_E is the eutectic concentration; $\Delta T = T_m - T_E$; L is the latent heat; and \hat{n} denotes the unit normal to the interface pointing into the liquid phase.

The model is closed with a Gibbs-Thompson interface condition of the form

$$T_I - T_{m_0} = mC_I + \frac{\sigma \kappa T_m}{L} + \frac{V}{\mu} \left(\frac{T_m (C_{p_\ell} - C_{p_s})}{L} \right) \left[T_I \ln \left(\frac{T_I}{T_m} \right) + T_m - T_I \right] \quad (6)$$

T_{m_0} and T_m are related through the liquidus line in the phase diagram by

$$T_m = T_{m_0} + mC_I \quad (7)$$

where m is the slope of the liquidus line, C_I is the local interface concentration, σ is the surface tension, κ is the local interface curvature, and μ is the kinetic mobility.

NUMERICAL METHOD

The equations are discretized using a Galerkin formulation with linear (1-D) or bilinear (2-D) elements. It suffices to consider two types of intersections with bilinear elements as shown in Fig. 1. In these elements, the mass matrix is integrated separately over each phase with the aid of two isoparametric transformations. This results in the exact mass distribution when the solid and liquid phases have different heat capacities.

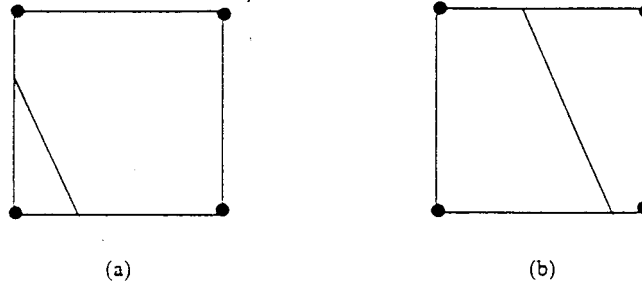


Fig. 1. Element intersected by an interface: (a) triangular; (b) quadrilateral.

Figure 2 illustrates the oscillating velocities that are typical of these simulations if the stiffness matrix is integrated exactly, as was done for the mass matrix. To resolve this problem, we utilize the equivalent diffusivity proposed by Patankar [7] in one dimension,

$$\alpha_{eq} = \frac{h\alpha_s\alpha_t}{(h-x_I)\alpha_s + x_I\alpha_t} \quad (8)$$

where h is the element size and x_I is the interface position. We have successfully extended the concept to two dimensions by applying it at every point in one spatial direction and then integrating in the other direction. This yields anisotropic equivalent conductivities in two and three dimensions.

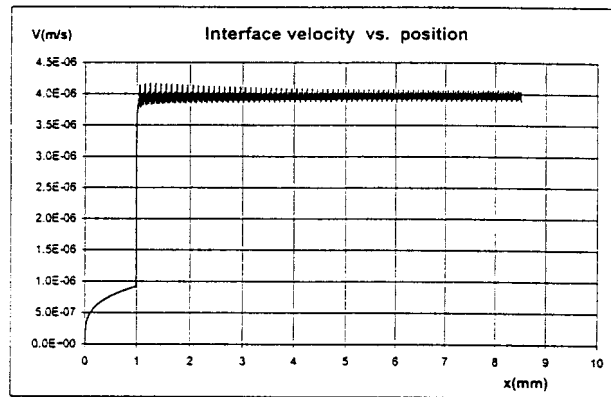


Fig. 2. Interface velocity versus position in one-dimensional solidification of a Pb-5.8wt%-Sb alloy showing oscillations.

The direction normal to the interface and the interface curvature are calculated at each marker point using a local quadratic interpolant centered at the marker. The distance between markers is kept between $0.3h < d < 0.9h$. If the distance becomes larger, a marker is added in between and, if it becomes shorter, a marker is taken out.

The interface position and velocity are calculated iteratively using the method depicted in Fig. 3. The quantity e_k is evaluated using Eq. (2b), where the derivatives are approximated using the temperatures T_1 and T_2 along the normal to the interface and h_m is chosen as $h_m = 1.5h$, guaranteeing that these points are not in the element containing the interface in the two-dimensional case. The same idea has been extended to a quadratic interpolant of the normal derivative using four points along the normal to ensure quadratic convergence.

EXAMPLES AND DISCUSSION

Error analysis of the current method will show only a linear convergence rate because of the lack of smoothness of the solution at the interface where the derivative of the temperature is discontinuous. However, we can show that the method is second-order accurate through detailed calculations performed in two cases involving a pure substance for which analytical solutions are available [8, 9]. The first is a one-dimensional problem in which the domain is at a uniform temperature larger than

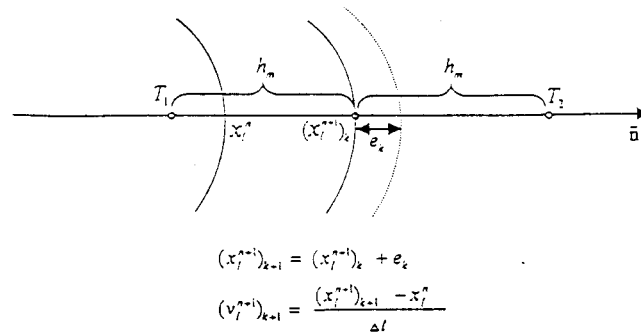


Fig. 3. Calculations of the current interface position and interface velocity.

T_m and at time $t = 0$ the temperature at the left-hand end is lowered below the freezing temperature. This was also solved in [10]. The second is an axisymmetric problem with a central sink that we solve as a two-dimensional problem in Cartesian coordinates. A typical result for the first such problem measuring the error in the location of the interface after 150,100 seconds of solidification, together with the data, is shown in Fig. 4 where the second-order convergence rate is evident.

The next example involves solidification of a Pb-22wt%-Sb alloy. In one dimension, the region length is $L_0 = 0.02$ m, an initial temperature gradient of 10,000 K/m is imposed with the temperature at $x = 0$ equal to the initial melting temperature $T_{m0} = 585.474$ K. This temperature gradient is applied at all times at $x = 0.02$ and at $t > 0$. A cooling rate of 0.03 K/s is imposed at $x = 0.0$. The rest of the material properties are $\rho_s = \rho_l = 10,190$ kg/m³, $D_l = 7.53 \times 10^{-10}$ m²/s, $k = 0.312$, $C_E = 11.2$ wt%, $T_E = 524$ K, $m = -6.83$, $L = 28,770$ J/kg, $C_{p_s} = 141$ J/kgK, $C_{p_l} = 151$ J/kgK, $\kappa_s = 20$ J/m \cdot s \cdot K, and $\kappa_l = 15$ J/m \cdot s \cdot K. Results obtained on a 200-element mesh for the temperature, a 200-element adaptive mesh for the solute concentration, and a time step $\Delta t = 0.25$ s are shown in Fig. 5. For

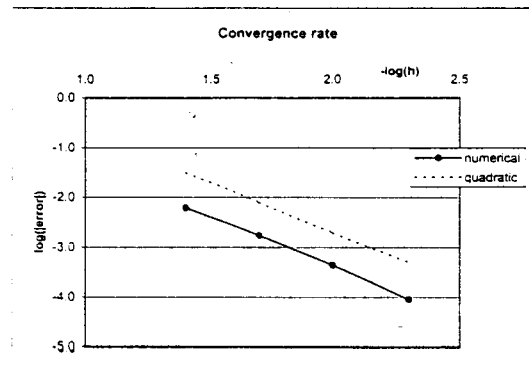


Fig. 4. Convergence rate of the interface location.

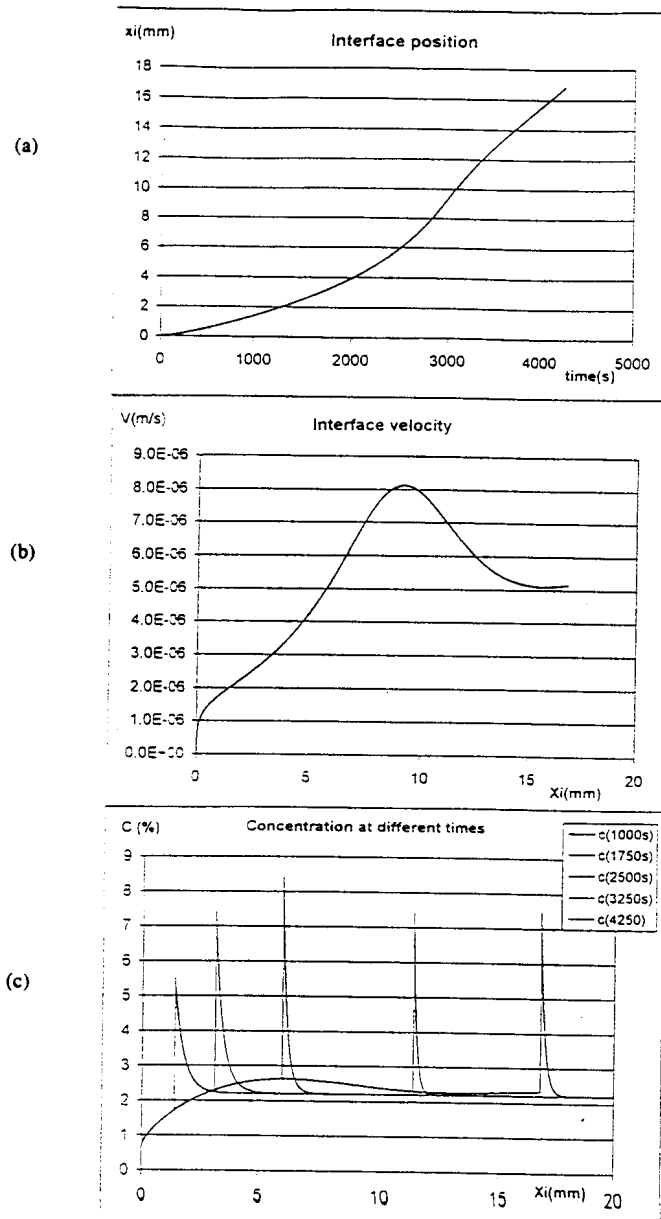


Fig. 5. Results for solidification of Pb-2.2wt%-Sb alloy: (a) interface position versus time; (b) interface velocity versus position; (c) interface concentrations at different times.

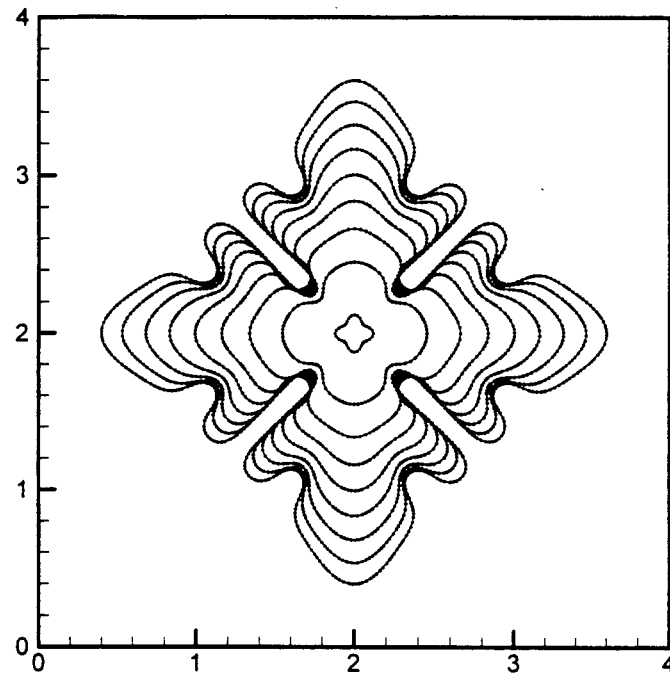


Fig. 6. Dendritic solidification into a supercooled melt; interface position at intervals of $\Delta t = 0.05$.

$C_0 = 2.2\text{wt\%}\text{-Sb}$, the eutectic concentration is not reached at the interface and therefore steady solidification is not achieved. Figure 5c shows the concentration profiles that show the sharp concentration boundary layer that forces us to use an adaptive mesh in the solution of the solute concentration equation. Unfortunately, we cannot discuss this in more detail here; for details, see [11].

Finally, we present an example of dendritic growth into an undercooled liquid. At the center of a square domain 4 units long and at uniform initial temperature lower than the melting temperature ($T_\infty < T_m$), we place a solid seed at temperature T_m specified by $x = x_c + R\cos\theta$, $y = y_c + R\sin\theta$, where (x_c, y_c) is the center of the square and $R = 0.1 + 0.02\cos 4\theta$. The undercooling $T_\infty - T_m$ is chosen so that $St = -0.5$ and $\sigma = \mu = 0.002$. The heat capacities are uniform and $\kappa_s = 1.0$, $\kappa_l = 0.1$. Results obtained in a 100-by-100 square mesh are shown in Fig. 6, where the innermost curve is the initial condition and the rest of the contours are the interface position at intervals $\Delta t = 0.05$.

These results cannot be compared to exact solutions. Two-dimensional cases similar to our last example compare very well with previously published results in some cases. However, in other cases, our solutions are very different. We also observe that in those cases where our solutions agree with previously published ones, we can obtain comparable accuracy in coarser meshes, typically with half the number of nodes in each direction. The extension of the two-dimensional model to include the solute conservation equation is currently being performed and will be reported in the near future.

ACKNOWLEDGMENTS

This work was partially supported by the National Aeronautics and Space Administration under grant NCC8-96#4. We also would like to thank Prof. D. R. Poirier for his continuous help and encouragement during the development of this model.

REFERENCES

- [1] Murray, B. T., Wheeler, A. A., and Glicksman, M. F., *Simulations of Experimentally Observed Dendritic Growth Behavior Using a Phase-Field Method*, J. Crystal Growth, Vol. 154, 1995, pp. 386-400.
- [2] Warren, J. A. and Boettinger, W. J., *Prediction of Dendritic Growth and Microsegregation Patterns in a Binary Alloy Using the Phase-Field Method*, Acta Metall. Mater., Vol. 43, 1995, pp. 689-703.
- [3] Juric, D. and Tryggvason, G., *A Front-Tracking Method for Dendritic Solidification*, J. Comp. Phys., Vol. 123, 1996, pp. 127-148.
- [4] Udaykumar, H. S., Mittal, R., and Shyy, W., *Computation of Solid-Liquid Phase Fronts in the Sharp Interface Limit on Fixed Grids*, J. Comp. Phys., Vol. 153, 1999, pp. 535-574.
- [5] Sullivan, J. M. and Lynch, D. R., *Non-Linear Simulation of Dendritic Solidification of an Undercooled Melt*, Int. J. Num. Meth. Eng., Vol. 25, 1988, pp. 415-444.
- [6] Provatas, N., Goldenfeld, N., and Dantzig, J., *Adaptive Mesh Refinement Computation of Solidification Microstructures Using Dynamic Data Structures*, J. Comp. Phys., Vol. 148, 1999, pp. 265-290.
- [7] Patankar, S., *Numerical Heat Transfer and Fluid Flow*, Hemisphere Publishing Co., Washington, 1980.
- [8] Carslaw, H. and Jaeger, J., *Conduction of Heat in Solids*, 2nd Edition, Clarendon Press, Oxford, 1959.
- [9] Alexiades, V. and Solomon, A. D., *Mathematical Modeling of Melting and Freezing Processes*, Hemisphere Publishing Co., Washington, 1993.
- [10] Crivelli, L. A. and Idelsohn, S. R., *A Temperature Based Finite Element Solution for Phase Change Problems*, Int. J. Num. Meth. Eng., Vol. 23, 1986, pp. 99-119.
- [11] Zhao, P., Heinrich, J. C., and Poirier, D. R., *Modeling Solidification Interfaces in a Binary Alloy: Part I*, Aerospace and Mechanical Engineering, The University of Arizona, Tucson, 2000.